intake was prohibited due to gastric bleeding before RT, four (50%) resumed oral intake after RT.

Survival analysis and adverse events

As shown in Figs. 3 and 4, the median EFS from the end of RT and the OS from the first day of RT were 1.5 and 3.4 months, respectively. For EFS, one patient underwent blood transfusion after RT because of anemia, which was supposed to be caused by the subsequent chemotherapy following RT. The median survival time of all patients from the first diagnosis was 12.7 months.

The observed adverse events presented in Table 3 show the frequent occurrence of hematological adverse events. However, most of the patients with grade 3–4 hypohemoglobinemia showed the same grade before, during and after RT. One patient who received chemoradiotherapy developed grade 3 leukocytopenia with no sign of infection. Although there were three patients with grade 3 anorexia (one patient underwent chemoradiation), all of them recovered immediately after completion of RT.

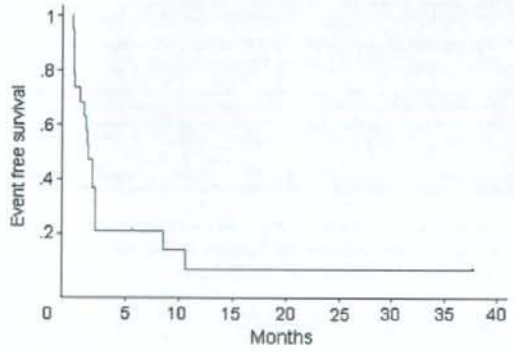

Fig. 3 Event-free survival from the day of completing radiation

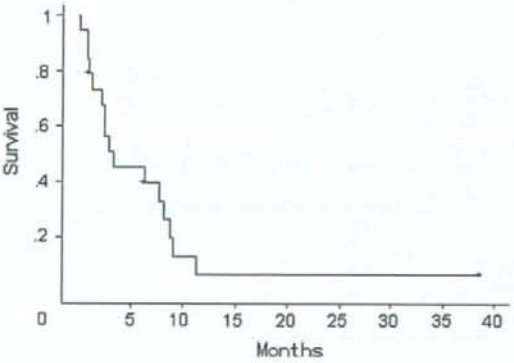

Fig. 4 Survival from the day of starting radiation

Table 3 Toxicity in patients receiving radiation

	Grade 1	Grade 2	Grade 3	Grade 4
Leukocyte	0	2	2[a]	0
Hemoglobin	0	4	9[b]	6[c]
Platelet	0	0	0	0
Anorexia	3	4	3	0
Nausea	3	1	1	0
Lethergy	3	2	0	0
Diarrhea	1	0	0	0
Dysphagia	0	1	0	0

[a] One patient received chemoradiation

[b] Ten patients had grade 3 hemoglobin at start of radiation

[c] Two patinets had grade 4 hemoglobin at start of radiation

Discussion

We confirmed here the efficacy of palliative RT in achieving hemostasis in patients with bleeding from gastric cancer. In our clinical experience, successful hemostasis was observed in 13 of 19 patients (68%), without severe adverse effects.

Several reports of palliative RT for local symptom control in patients with unresectable or metastatic gastric cancer are found in the literature. Moreover, several investigators have applied RT for the palliation of obstructive symptoms. Mantell (1982) reported that palliative RT improved dysphasia in 13 of 17 patients (76%). Coia et al. (1998) showed that a combination of RT, fluorouracil and mitomycin successfully relieved dysphasia in six of nine patients (67%). More recently, Kim et al. (2007) have reported that 13 (81%) of 16 patients with dysphasia/obstruction positively responded to RT.

For bleeding control, Tey et al. (2007) reported that 13 of 24 patients (54%) with bleeding from gastric cancer were responsive to RT. However, they simply defined a positive response as improvement or stabilization of the Hb level without providing any discussion on blood transfusion. Kim et al. (2007) have also reported that palliative RT was successful in achieving hemostasis in 14 (70%) of 20 patients. Bleeding was controlled for a median of 11.4 months, which corresponded to 81% of the patients' remaining life (Kim et al. 2007).

In the present analysis, we defined treatment success as absence of the need for blood transfusion for more than 1 month after RT without any other cause of death. Our results are comparable with those of previous reports. We also demonstrated the median duration of sustained

efficacy; however, the median EFS of 1.5 months here was shorter than that of Kim's report. This can be explained by the difference in the definition of treatment success and cohort differences. We believe that the cohort of this study has limited survival when RT was conducted. Interestingly, Kim et al. simply defined treatment success as the absence of the need for coagulation, or no compliant of symptoms during follow up; however, they made no mention about blood transfusion. Here, the median OS was 3.4 months, also shorter than those reported by Tey et al. (2007) and Kim et al. (2007). Most patients analyzed here had poor PS with severe bleeding, and all of them were classified as stage IV and thus ineligible for operation. Moreover, heterogeneous patients who presented with not only bleeding but also stenosis or pain were included in the analysis in previous reports (Kim et al. 2007; Tey et al. 2007).

The reported palliative RT doses for unresectable gastric cancer range widely from 8 to 60 Gy. Tey et al. found no dose–response relationship between responders and non-responders ($P = 0.078$), whereas Kim et al. suggested that a BED of 41 Gy_{10} or more was correlated with better local symptom control ($P = 0.05$). Our data demonstrated a significant dose–response relationship between BEDs of 50 Gy_{10} or more and <50 Gy_{10} ($P = 0.040$). These results are based on the fact that only patients with bleeding were analyzed, and our definition of hemostasis was a clearer objective endpoint than that of other reports. In our experience, successful hemostasis was observed in as high as 91% of patients who completed an initial planned dose (mostly 40 Gy in 16 fractions: BED of 50 Gy_{10}). Despite this relatively high dose, toxicities were tolerable in most patients similarly to other reports (Kim et al. 2007; Tey et al. 2007).

Kim et al. suggested that a lower RT dose (BED <41 Gy) correlated with poor local control (56 and 70%), while Tey et al. found no evidence suggestive of a dose–response relationship. Most patients received a BED of 39 Gy_{10}, which corresponds to a dose of 30 Gy in ten fractions. Thus, different cut-off points may produce different result from ours.

It remains a matter of debate whether gastrectomy for preventing mortality from local progression can improve survival of patients with metastatic gastric cancer. A previous cohort study has shown that only 7% of gastric cancer patients with metastases not undergoing gastrectomy needed intervention due to bleeding (Sarela et al. 2007). Their median survival time was similar to those of a previous series of patients undergoing gastrectomy. A clinical trial is now underway in Japan and Korea to compare the effects of chemotherapy following gastrectomy with the effects of chemotherapy without gastrectomy in patients with metastatic gastric cancer.

Because of the retrospective nature of the present analysis, there are a number of study limitations that may have affected the interpretation of our findings. The dose used in our facility may not always be valid in other facilities because the best available dose has not yet been established. Also, patient population was not homogenous because palliative RT was not used for initial treatment in most cases. Moreover, patients with gastric cancer who presented with bleeding after the failure of several chemotherapeutic regimens might be more resistant to palliative RT. Additionally, those showing good PS with less bleeding could easily complete the total planned dose, and thus may easily be considered as treatment success. On the other hand, those with pronounced bleeding could hardly complete the planned dose. In the present study, the treatment failure group included patients who discontinued the irradiation course because of deterioration of general condition. The dose–response relationships in our study might also be biased. Further studies in large number of patients are warranted to elucidate the appropriate dose for the palliation of bleeding from gastric cancer.

In conclusion, palliative RT was shown to be a powerful treatment of choice for achieving hemostasis in patients with bleeding from gastric cancer. Successful hemostasis was achieved in as high as 91% of patients who completed the initial planned dose (mostly 40 Gy in 16 fractions). A BED of 50 Gy_{10} or more was significantly correlated with treatment success compared with a BED of <50 Gy_{10} ($P = 0.040$). We recommend 40 Gy in 16 fractions for palliating bleeding from gastric cancer according to our analysis. Palliative RT is considered to be helpful not only in rendering transfusion unnecessary but also in re-starting oral nutrition, as well as in potentiating a positive response to other chemotherapy regimens.

References

Coia LR, Paul AR, Engstorm PF (1988) Combined radiation and chemotherapy as primary management of adenocarcinoma of esophagus and gastroesophageal junction. Cancer 61:643–649. doi:10.1002/1097-0142(19880215)61:4<643::AID-CNCR2820610404>3.0.CO;2-4

Encarnacion CE, Kadir S, Beam CA, Payne CS (1992) Gastrointestinal bleeding: treatment with gastrointestinal arterial embolization. Radiology 183:505–508

Ferris FD, Bezjak A, Rosenthal SG (2001) The palliative uses of radiation therapy in surgical oncology patients. Surg Oncol Clin N Am 10:185–201

Glimelius B, Hoffman K, Haglund U, Nyrén O, Sjödén PO (1994) Initial or delayed chemotherapy with best supportive care in advanced gastric cancer. Ann Oncol 5:189–190

Hoskin PJ (1998) Radiotherapy in symptom management. In: Doyle D, Hanks GWC, Macdonald N (eds) Oxford textbook of

palliative medicine, 2nd edn. Oxford University Press, New York, pp 278–280

Kamangar F, Dores GM, Anderson WF (2006) Patterns of cancer incidence, mortality, and prevalence across five continents: defining priorities to reduce cancer disparities in different geographic regions of the world. J Clin Oncol 24:2137–2150. doi:10.1200/JCO.2005.05.2308

Kaplan EL, Meier P (1958) Nonparametric estimation from incomplete observations. J Am Stat Assoc 53:457–481. doi:10.2307/2281868

Kim MM, Rana V, Janjan NA, Das P, Phan AT, Delclos ME, Mansfield PF, Ajani JA, Crane CH, Krishnan S (2007) Clinical benefit of palliative radiation therapy in advanced gastric cancer. Acta Oncol 47:421–427. doi:10.1080/02841860701621233

Loftus EV, Alexander GL, Ahlquist DA, Balm RK (1994) Endoscopic treatment of major bleeding from advanced gastroduodenal malignant lesions. Mayo Clin Proc 69:736–740

Mantell BS (1982) Radiotherapy for dysphagia due to gastric carcinoma. Br J Surg 69:69–70. doi:10.1002/bjs.1800690203

Murad AM, Santiago FF, Petroianu A, Rocha PR, Rodrigues MA, Rausch M (1993) Modified therapy with 5-fluorouracil, doxorubicin, and methotrexate in advanced gastric cancer. Cancer 72:37–41. doi:10.1002/1097-0142(19930701)72:1<37::AID-CNCR2820720109>3.0.CO;2-P

Ohtsu A, Yoshida S, Nagahiro S (2006) Disparities in gastric cancer chemotherapy between the East and West. J Clin Oncol 24:2188–2196. doi:10.1200/JCO.2006.05.9758

Onsrud M, Hagen B, Strickert T (2001) 10-Gy single-fraction pelvic irradiation for palliation and life prolongation in patients with cancer of cervix and corpus uteri. Gynecol Oncol 82:167–171. doi:10.1006/gyno.2001.6233

Pereira J, Phan T (2004) Management of bleeding in patients with advanced cancer. Oncologist 9:561–570. doi:10.1634/theoncologist.9-5-561

Pyrhönen S, Kuitunen T, Nyandoto P, Kouri M (1995) Randomized comparison of fluorouracil, epidoxorubicin and methotrexate (FEMTX) plus best supportive care alone in patients with non-resectable gastric cancer. Br J Cancer 71:587–591

Sarela AI, Yelluri S, Leeds Upper Gastrointestinal Cancer Multidisciplinary Team (2007) Gastric adenocarcinoma with distant metastasis: is gastrectomy necessary? Arch Surg 142:143–149. doi:10.1001/archsurg.142.2.143

Savides TJ, Jensen DM, Cohen J, Randall GM, Kovacs TOG, Pelayo E, Cheng S, Jensen ME, Hsieh H (1996) Severe upper gastrointestinal tumor bleeding: endoscopic findings, treatment and outcome. Endoscopy 28:244–248. doi:10.1055/s-2007-1005436

Srivastava DN, Gandhi D, Julka PK, Tandon RK (2000) Gastrointestinal hemorrhage in hepatocellular carcinoma: management with transhepatic arterioembolization. Abdom Imaging 25:380–384. doi:10.1007/s002610000056

Tey J, Back MF, Shakespeare TP, Mukherjee RK, Lu JJ, Lee KM, Wong LC, Leong CN, Zhu M (2007) The role of palliative radiation therapy in symptomatic locally advanced gastric cancer. Int J Radiat Oncol Biol Phys 67:385–388. doi:10.1016/j.ijrobp.2006.08.070

Urethral Dose and Increment of International Prostate Symptom Score (IPSS) in Transperineal Permanent Interstitial Implant (TPI) of Prostate Cancer

Naoya Murakami[1,2], Jun Itami[1,2], Kae Okuma[1], Hiroshi Marino[1], Keiichi Nakagawa[3], Tsukasa Ban[1], Moritoshi Nakazato[1], Kazuyoshi Kanai[1], Kuniji Naoi[1], Masashi Fuse[1]

Purpose: To find the factors which influence the acute increment of International Prostate Symptom Score (IPSS) after transperineal permanent interstitial implant (TPI) using ^{125}I seeds.

Patients and Methods: From April 2004 through September 2006, 104 patients with nonmetastatic prostate cancer underwent TPI without external-beam irradiation. Median patient age was 70 years with a median follow-up of 13.0 months. 73 patients (70%) received neoadjuvant hormone therapy. The increment of IPSS was defined as the difference between pre- and postimplant maximal IPSS. Clinical, treatment, and dosimetric parameters evaluated included age, initial prostate-specific antigen, Gleason Score, neoadjuvant hormone therapy, initial IPSS, post-TPI prostatic volume, number of implanted seeds, prostate V_{100}, V_{150}, D_{90}, urethral D_{max}, and urethral D_{90}. In order to further evaluate detailed urethral doses, the base and apical urethra were defined and the dosimetric parameters were calculated.

Results: The IPSS peaked 3 months after TPI and returned to baseline at 12–15 months. Multivariate analysis demonstrated a statistically significant correlation of post-TPI prostatic volume, number of implanted seeds, and the dosimetric parameters of the base urethra with IPSS increment.

Conclusion: The base urethra appears to be susceptible to radiation and the increased dose to this region deteriorates IPSS. It remains unclear whether the base urethral dose relates to the incidence of late urinary morbidities.

Key Words: Prostate cancer · International Prostate Symptom Score (IPSS) · Seed implant · ^{125}I · Urethral dose

Strahlenther Onkol 2008;184:515–9
DOI 10.1007/s00066-008-1833-3

Urethraldosis und Erhöhung des International Prostate Symptom Score (IPSS) bei transperinealer permanenter interstitieller Brachytherapie des Prostatakarzinoms

Ziel: Ermittlung von Parametern, die nach einer transperinealen permanenten interstitiellen Brachytherapie der Prostata mit ^{125}I eine Zunahme des International Prostate Symptom Score (IPSS) bewirken.

Patienten und Methodik: Von April 2004 bis September 2006 erhielten 104 Patienten mit nichtmetastasiertem Prostatakarzinom eine alleinige transperineale permanente interstitielle Brachytherapie mit ^{125}I ohne vorherige perkutane Therapie. Das mittlere Patientenalter betrug 70 Jahre, die mediane Beobachtungszeit lag bei 13,0 Monaten. 73 Patienten (70%) erhielten eine neoadjuvante Hormontherapie. Die Erhöhung des IPSS wurde als Differenz zwischen initialem und maximalem IPSS definiert. Analysiert wurden klinische, therapeutische sowie dosimetrische Parameter wie Patientenalter, initialer PSA-Wert (prostataspezifisches Antigen), Gleason-Score, neoadjuvante Hormontherapie, initialer IPSS, Prostatavolumen nach Implantation, Zahl der implantierten ^{125}I-Seeds, die DVH-Parameter V_{100}, V_{150}, D_{90} für die Prostata sowie D_{max} und D_{90} für die Urethra. Zur detaillierten Untersuchung der Urethrabelastung wurden basale und apikale Urethra definiert, für die ebenfalls DVH-Parameter berechnet wurden.

Ergebnisse: Der IPSS erreichte 3 Monate nach ^{125}I-Implantation sein Maximum und kehrte nach 12–15 Monaten wieder auf den Ausgangswert zurück. Eine multivariate Analyse ergab, dass das Prostatavolumen nach Implantation, die Anzahl der implantierten ^{125}I-Seeds und die dosimetrischen Parameter der Basisurethra statistisch signifikant mit der Erhöhung des IPSS korrelierten.

[1] Department of Radiation Therapy and Oncology, International Medical Center of Japan, Tokyo, Japan,
[2] Division of Radiation Therapy, National Cancer Center Hospital, Tokyo, Japan,
[3] Department of Radiology, School of Medicine, Tokyo University, Japan.

Received: January 11, 2008; accepted: July 3, 2008

Schlussfolgerung: Die basale Urethra scheint sich als strahlenempfindlich zu erweisen, und die erhöhte Dosis in dieser Region verschlechtert den IPSS. Unklar bleibt, ob die Dosis in der basalen Urethra im Zusammenhang mit dem Auftreten urethraler Spätwirkungen steht.

Schlüsselwörter: Prostatakarzinom · International Prostate Symptom Score (IPSS) · Seed-Implantat · ^{125}I · Urethradosis

Introduction

In the current management with radiotherapy for localized adenocarcinoma of prostate, intensity-modulated radiotherapy [6] and ultrasound-guided transperineal permanent interstitial implant (TPI) using ^{125}I radioactive seeds [2] are widely employed, because both methods satisfy the requirement of dose escalation to achieve biochemical control and reduce dose to the normal tissues. With the clinical experiences accumulated for decades, guidelines on standardized TPI for localized prostate cancer were established [9, 16] and favorable long-term results were achieved [5, 14, 15, 18]. In TPI, acute urinary morbidities are seen in most of the patients and this is reflected in the increment of International Prostate Symptom Score (IPSS). However, introduction of the peripheral or modified peripheral seed placement methods has reduced urethral dose dramatically and the relationship between the urethral dose and the increment of IPSS has been variously reported. In the present study, the detailed urethral doses of TPI were investigated in relation to the acute increment of IPSS.

Patients and Methods

From April 2004 through September 2006, 104 patients with nonmetastatic prostate cancer underwent TPI with documentation of the IPSS before and after the procedure. Patients treated with combined external-beam radiation therapy were excluded from this study. Clinical characteristics of the 104 patients are summarized in Table 1. T-stage according to the International Union Against Cancer (UICC) [17] was defined solely by digital rectal examination without considering information of the radiologic images. We stratified patients according to the Seattle risk classification [18]. The number of patients who received neoadjuvant hormone therapy was 73 (70%) and most of them were started by urologists. Neoadjuvant hormone therapy consisted of antiandrogen in 29 (40%), LHRH (luteinizing hormone-releasing hormone) agonist in eight (11%), and maximum androgen blockade in 36 (49%). Median duration of each neoadjuvant hormone therapy was 5 months, 13 months, and 8.5 months for antiandrogen, LHRH agonist, and maximum androgen blockade, respectively. Adjuvant hormone therapy was not performed in this series.

The TPI was performed exclusively with ^{125}I seeds (OncoSeed, MediPhysics, Kobe, Japan) of 0.394 mCi (14.6 MBq) or 0.385 mCi (14.2 MBq). About 3 weeks before the implant, prostate volumetry by axial transrectal ultrasound (TRUS; ProSound 4000, Aloka, Tokyo, Japan) with 5-mm intervals was performed with a Foley catheter in place. The TRUS was mounted on the stepper (AccuSeed, CMS, St. Louis, MO, USA). The prostate contour (= clinical tumor volume) was extracted and stored in VariSeed version 7.01 (Varian, Palo Alto, CA, USA) and 3-mm margins were placed around the clinical tumor volume to construct the planning target volume (PTV) in all directions except in the rectal direction, where no margin was added to reduce the rectal dose. In the preplanning, ^{125}I seeds were placed with the modified peripheral loading to deliver 145 Gy to the PTV. The TPI was performed under epidural anesthesia and ^{125}I seeds were implanted by Mick Applicator™ (Mick Radionuclear, Mount Vernon, NY, USA) through the appropriate template holes according to the preplanning with intraoperative modifications.

1 month after the TPI, final postplanning dosimetry was performed in all patients, because it has been reported that the prostate volume increases by trauma-associated fluid accumulation and bleeding within the gland immediately after the implantation [9, 13, 16]. A computed tomography (CT) image

Table 1. Patient characteristics. PSA: prostate-specific antigen.

Tabelle 1. Patientencharakteristik. PSA: prostataspezifisches Antigen.

	Patients n (%)
Age (years), median (range)	70.0 (48–82)
Stage	
• T1c	73 (70)
• T2a	12 (12)
• T2b	6 (6)
• T2c	10 (10)
• T3a	2 (2)
• T3b	1 (1)
Initial PSA (ng/ml), mean	12.2
• < 10	67 (64)
• 10–20	22 (21)
• > 20	15 (14)
Gleason Score	
• < 7	66 (63)
• 7	27 (26)
• > 7	11 (11)
Risk grouping	
• Low	36 (35)
• Intermediate	48 (46)
• High	20 (19)
Neoadjuvant hormone therapy	73 (70)
Follow-up (months), median (range)	13.0 (2–34)

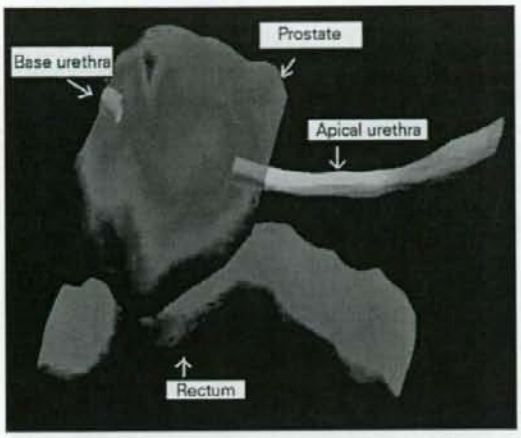

Figure 1. Definitions of base and apical urethras.

Abbildung 1. Definitionen der basalen und apikalen Urethra.

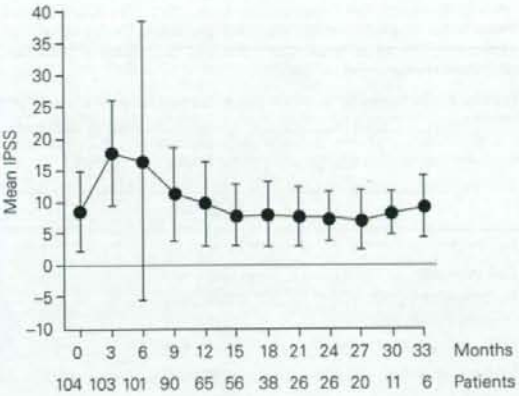

Figure 2. Change of mean International Prostate Symptom Scores (IPSS) after transperineal permanent interstitial implant (TPI). The figures shown in the lowest row represent the number of patients assessable. Error bars represent standard deviations.

Abbildung 2. Zeitliche Veränderung der durchschnittlichen International Prostate Symptom Scores (IPSS) nach transperinealer permanenter interstitieller Brachytherapie. Die Ziffern in der unteren Reihe entsprechen der auswertbaren Patientenzahl im jeweiligen Zeitintervall. Die Fehlerbalken zeigen die Standardabweichungen.

was taken with 2- or 3-mm intervals. T2-weighted magnetic resonance (MR) images were fused with the CT images to help extract the prostate contour. CT and MR images were obtained with a Foley catheter in place. Dose calculation was performed with the VariSeed™. The urethral dose was calculated at the outer rim of the Foley catheter from the bladder neck to the CT slice where the most caudally located seed can be found. In all patients, an α-blocker was prescribed from the day following TPI until subsidence of urinary symptoms.

The increment of IPSS was defined as the difference between the preimplant IPSS and the maximal IPSS after the implant. Postimplant IPSS was evaluated in the 1st and 4th weeks after the implant, and then every 2–3 months.

Various patient, tumor, and treatment factors as well as the TPI dosimetric factors were analyzed to find statistically significant relationships with the increment of IPSS. For calculation of the prostate volume, an MR image taken at the time of postplanning was used. D_{90} indicates the minimal dose covering 90% of the prostate expressed in Gray, V_{100} and V_{150} represent volume ratio of the prostate receiving at least 100% and 150% of the prescribed dose, respectively. The urethral D_{max} (maximal dose) and urethral D_{90} (minimal dose covering 90% of the entire prostatic urethra) were also calculated. In addition, base and apical urethras were extracted from the postplanning CT. The base urethra is defined as the most proximal 2–3 mm long portion of the prostatic urethra (actually, contouring two slices of CT images) neighboring the bladder neck (Figure 1). The apical urethra is apical 6 mm of the prostatic urethra. For the base and apical urethras, the D_{max}, D_{50} (minimal dose covering 50% of the corresponding structure), and D_{90} were calculated.

The relationships between clinical and treatment variables and the increment of IPSS were analyzed by univariate analysis. The continuous variables were dichotomized to give the lowest p-values in the t-test, where the increment of IPSS score was considered continuous. The variables with p-values < 0.05 were further analyzed in multivariate analysis by logistic regression models. In the multivariate analysis, the patients were dichotomized by the mean increment of IPSS into the larger and smaller increments, while the clinical and treatment variables were treated as continuous.

Results

The time course of mean IPSS change after TPI every 3 months is shown in Figure 2 with the respective number of patients. The IPSS reached its maximum 3 months after the implant and decreased gradually until 15 months. The increment of IPSS after the implant ranged from –9 to 31 with a mean of 10.7.

The mean IPSS before TPI was 8.5, and the number of seeds implanted ranged from 40 to 114 with a mean of 71.3 (Table 2). Total activity of the implanted seeds ranged from 15.4 to 45.9 mCi (0.57–1.70 GBq). The mean prostate volume evaluated in post-TPI MR images was 22.9 ml. Prostate V_{100} ranged from 51.9% to 99.8% of the prostate volume, and in 62 of the 104 patients the prostate V_{100} of $\geq 90\%$ was attained.

Table 2. Treatment and dosimetric characteristics. IPSS: International Prostate Symptom Score; SD: standard deviation; TPI: transperineal permanent interstitial implant. For detailed definitions of the dosimetric parameters refer to the text.

Tabelle 2. Therapeutische und dosimetrische Charakteristika. IPSS: International Prostate Symptom Score; SD: Standardabweichung; TPI: transperineale permanente interstitielle Brachytherapie. Genaue Definitionen der dosimetrischen Parameter finden sich im Text.

	Mean (SD)
Pre-TPI IPSS	8.5 (6.2)
IPSS increment	10.7 (6.9)
Prostate volume (ml)	22.9 (8.4)
Implanted seeds (n)	71.3 (13.6)
Seed activity (mCi)	28.2 (5.8)
Seed activity (GBq)	1.04 (0.21)
Prostate V_{100} (%)	89.5 (8.2)
Prostate V_{150} (%)	55.5 (14.3)
Prostate D_{90} (Gy)	147.2 (27.4)
Urethra D_{max} (Gy)	239.5 (55.7)
Urethra D_{90} (Gy)	100.5 (31.2)
Apical urethra D_{max} (Gy)	219.9 (43.2)
Apical urethra D_{90} (Gy)	100.8 (34.1)
Apical urethra D_{50} (Gy)	166.0 (36.5)
Base urethra D_{max} (Gy)	162.4 (43.3)
Base urethra D_{90} (Gy)	116.0 (31.7)
Base urethra D_{50} (Gy)	134.6 (34.5)

Table 3. Results of the univariate analysis to demonstrate the influence of clinical and dosimetric variables upon the increment of International Prostate Symptom Score (IPSS). PSA: prostate-specific antigen. For detailed definitions of the dosimetric parameters refer to the text.

Tabelle 3. Ergebnisse der univariaten Analyse, die den Einfluss der klinischen und dosimetrischen Varianten auf die Zunahme des International Prostate Symptom Score (IPSS) zeigen. PSA: prostataspezifisches Antigen. Genaue Definitionen der dosimetrischen Parameter finden sich im Text.

Variables		p-value
Age (years)	(≥ 73 years vs. < 73 years)	0.0039
PSA (ng/ml)	(≥ 20 ng/ml vs. < 20 ng/ml)	0.0100
Gleason Score	(≥ 7 vs. < 7)	0.67
Preimplant IPSS	(≥ 7 vs. < 7)	0.10
Prostate volume (ml)	(≥ 20 ml vs. < 20 ml)	< 0.0001
Implanted seeds (n)	(≥ 65 vs. < 65)	0.0017
Neoadjuvant hormone therapy	(+ vs. −)	0.0508
Prostate V_{100} (%)	(≥ 90% vs. < 90%)	0.0102
Prostate V_{150} (%)	(≥ 50% vs. < 50%)	0.0644
Prostate D_{90} (Gy)	(≥ 145 Gy vs. < 145 Gy)	0.0075
Urethra D_{max} (Gy)	(≥ 290 Gy vs. < 290 Gy)	0.5351
Urethra D_{90} (Gy)	(≥ 87 Gy vs. < 87 Gy)	0.1881
Apical urethra D_{max} (Gy)	(≥ 261 Gy vs. < 261 Gy)	0.4078
Apical urethra D_{90} (Gy)	(≥ 87 Gy vs. < 87 Gy)	0.3675
Apical urethra D_{50} (Gy)	(≥ 145 Gy vs. < 145 Gy)	0.5147
Base urethra D_{max} (Gy)	(≥ 188.5 Gy vs. < 188.5 Gy)	0.0003
Base urethra D_{90} (Gy)	(≥ 116 Gy vs. < 116 Gy)	0.0044
Base urethra D_{50} (Gy)	(≥ 116 Gy vs. < 116 Gy)	0.0015

Mean prostate D_{90} was 147.2 Gy with 61 patients showing the value ≥ 145 Gy. The urethral D_{max} was higher in the apical urethra as compared to the base urethra.

Univariate analysis of the various parameters and the increment of IPSS revealed that age, initial PSA, post-TPI prostatic volume, number of seeds implanted, prostate V_{100} and D_{90}, D_{max}, and D_{90} and D_{50} of the base urethra were statistically significantly related to the IPSS increment (Table 3). These parameters were further examined in a multivariate analysis, which demonstrated that the increment of IPSS correlated with the postimplant prostatic volume, number of implanted seeds, and the dosimetric parameters of the base urethra (Table 4). A higher dose to the base urethra caused a more unfavorable acute IPSS increment.

Discussion

As we experienced only one patient with acute urinary retention after TPI during this time period, we confined our analysis to the increment of IPSS as an acute urinary morbidity. Like other studies using ^{125}I, our study demonstrated that the IPSS increased maximally around 3 months after TPI and returned to the pretreatment level at about 12 months [2, 11]. There are several clinical as well as dosimetric parameters reported to correlate with the urinary morbidities after TPI. In the present study, the prostatic volume and the number of implanted seeds show a statistically significant relation to the increment of IPSS. Kelly et al. [7] and Bottomley et al. [3] also found an influence of prostatic volume and number of implanted seeds upon the increment of IPSS. Additionally, pretreatment IPSS [3, 7, 10], pretreatment urinary flow [19], number of needles used for seed implant [3, 8], and neoadjuvant hormone therapy [4] have been reported to be related to the increment of IPSS. Although it is rational to assume that urethral dose is related to the increment of IPSS, the relationship between them remains quite controversial. Our study revealed that the dosimetric parameters of the base urethra have a statistically significant impact upon the increment of IPSS. Similarly, Williams et al. found a relationship between increment of IPSS and the number of seeds above the prostatic base [19]. They consider the number of seeds above the prostatic base to reflect the dose to the bladder neck and trigone which may be sensitive to radiation. Pinkawa et al. suggested that the seminal vesicle dose is closely related to the dose to the bladder neck and the urethral sphincter muscle and late urinary dysfunction is more frequent in patients with a higher seminal vesicle dose [12]. By contrast, Allen et al. could not find sig-

Table 4. Results of the multivariate analysis to demonstrate the influence of clinical and treatment variables upon the increment of International Prostate Symptom Score (IPSS). MRI: magnetic resonance imaging; PSA: prostate-specific antigen. For detailed definitions of the dosimetric parameters refer to the text.

Tabelle 4. Ergebnisse der multivariaten Analyse, die den Einfluss der klinischen und dosimetrischen Varianten auf die Zunahme des International Prostate Symptom Score (IPSS) zeigen. MRI: Magnetresonanztomographie; PSA: prostataspezifisches Antigen. Genaue Definitionen der dosimetrischen Parameter finden sich im Text.

Variables	p-value
Age (years)	0.9033
PSA (ng/ml)	0.1901
MRI volume (ml)	0.0006
Seed	0.0151
Prostate V_{100} (Gy)	0.9123
Prostate D_{90} (Gy)	0.2841
Base urethra D_{max} (Gy)	0.0530
Base urethra D_{90} (Gy)	0.0151
Base urethra D_{50} (Gy)	0.0095

nificant relationships between various segmental urethral dose parameters and time to the resolution of IPSS increment, although they showed the maximal IPSS is related to the maximal apical urethral dose [1]. They segmented the prostatic urethra into base, midgland and apex each with 1 cm length, while our study limited base urethra only to the proximal 2–3 mm of prostatic urethra, which might have disclosed the sensitivity of this tiny region or bladder neck to radiation.

In this retrospective analysis, the patients included had been treated at the very initial phase after the introduction of TPI in our department. Therefore, in some patients the optimal quality of seed implantation was not attained and urethral dose reached < 100% of the prescribed dose. Although it is required to deliver an adequate dose to sterilize tumor cells around the base urethra, severity of the acute urinary morbidities represented by the increment of IPSS seems to be lowered by reducing the dose to the base urethra toward the prescribed dose.

Conclusion

The base urethra or bladder neck appears to be susceptible to radiation and the increased dose to this region acutely deteriorates IPSS. It remains unclear whether the radiation dose to this region relates to the incidence of late urinary morbidities.

References

1. Allen ZA, Merrick GS, Butler WM, et al. Detailed urethral dosemetry in the evaluation of prostate brachytherapy-related urinary morbidity. Int J Radiat Oncol Biol Phys 2005;62:981–7.
2. Block T, Czempiel H, Zimmermann F. Transperineal permanent seed implantation of "low-risk" prosate cancer. Strahlenther Onkol 2006;182:666–71.
3. Bottomley D, Ash D, Al-Qaisieh B, et al. Side effects of permanent I125 prostate seed implants in 667 patients treated in Leeds. Radiother Oncol 2007;82:46–9.
4. Crook J, McLean M, Catton C, et al. Factors influencing risk of acute urinary retention after TRUS-guided permanent prostate seed implantation. Int J Radiat Oncol Biol Phys 2002;52:453–60.
5. Grimm PD, Blasko JC, Sylvester JE, et al. 10-year biochemical (prostate-specific antigen) control of prostate cancer with ^{125}I brachytherapy. Int J Radiat Oncol Biol Phys 2001;51:31–40.
6. Guckenberger M, Flentje M. Intensity-modulated radiotherapy (IMRT) of localized prostate cancer. Strahlenther Onkol 2007;183:57–62.
7. Kelly K, Swindell R, Routledge J, et al. Prediction of urinary symptoms after 125-iodine prostate brachytherapy. Clin Oncol (R Coll Radiol) 2006; 18:326–32.
8. Keyes M, Schellenberg D, Moravan V, et al. Decline in urinary retention incidence in 805 patients after prostate brachytherapy: the effect of learning curve? Int J Radiat Oncol Biol Phys 2006;64:825–34.
9. Nag S, Bice W, DeWyngaert K, et al. The American Brachytherapy Society recommendations for permanent prostate brachytherapy post-implant dosimetric analysis. Int J Radiat Oncol Biol Phys 2000;46:221–30.
10. Niehaus A, Merrick GS, Butler WM, et al. The influence of isotope and prostate volume on urinary morbidity after prostate brachytherapy. Int J Radiat Oncol Biol Phys 2006;64:136–43.
11. Ohashi T, Yorozu A, Toya K, et al. Serial changes of international prostate symptom score following I-125 prostate brachytherapy. Int J Clin Oncol 2006;11:320–5.
12. Pinkawa M, Fischedick K, Piroth MS, el al. Health-related quality of life after permanent interstitial brachytherapy for prostate cancer. Strahlenther Onkol 2006;182:660–5.
13. Pinkawa M, Gagel B, Piroth MD, et al. Changes of dose delivery distribution within the first month after permanent interstitial brachytherapy for prostate cancer. Strahlenther Onkol 2006;182:525–30.
14. Potters L, Morgenstern C, Calugaru E, et al. 12-year outcomes following permanent prostate brachytherapy in patients with clinically localized prostate cancer. J Urol 2005;173:1562–6.
15. Ragde H, Korb LJ, Elgamal AA, et al. Modern prostate brachytherapy. Prostate specific antigen results in 219 patients with up to 12 years of observed follow-up. Cancer 2000;89:135–41.
16. Salembier C, Lavagnini P, Nickers P, et al. Tumor and target volumes in permanent prostate brachytherapy: a supplement to the ESTRO/EAU/EORTC recommendations on prostate brachytherapy. Radiother Oncol 2007;83:3–10.
17. Sobin LH, Wittekind C, eds. TNM classification of malignant tumors, 6th edn. New York: Wiley-Liss, 2002.
18. Sylvester JE, Blasko JC, Grimm PD, et al. Ten-year biochemical relapse-free survival after external beam radiation and brachytherapy for localized prostate cancer: the Seattle experience. Int J Radiat Oncol Biol Phys 2003;57:944–52.
19. Williams SG, Millar JL, Duchesne GM, et al. Factors predicting for urinary morbidity following ^{125}iodine transperineal prostate brachytherapy. Radiother Oncol 2004;73:33–8.

Address for Correspondence
Jun Itami, MD
Division of Radiation Therapy
National Cancer Center Hospital
5-1-1 Tsukiji, Chuo-ku
Tokyo, 104-0045
Japan
Phone (+81/3) 354-22511, Fax -53567
e-mail: jitami@ncc.go.jp

Int. J. Radiation Oncology Biol. Phys., Vol. 72, No. 5, pp. 1347–1354, 2008

0360-3016/08/$–see front matter

ELSEVIER

doi:10.1016/j.ijrobp.2008.03.055

CLINICAL INVESTIGATION **Brain**

SPINAL RECURRENCE FROM INTRACRANIAL GERMINOMA: RISK FACTORS AND TREATMENT OUTCOME FOR SPINAL RECURRENCE

KAZUHIKO OGAWA, M.D.,* YOSHIHIKO YOSHII, M.D.,† NAOTO SHIKAMA, M.D.,‡ KATSUMASA NAKAMURA, M.D.,§ TAKASHI UNO, M.D.,‖ HIROSHI ONISHI, M.D.,¶ JUN ITAMI, M.D.,** YOSHIYUKI SHIOYAMA, M.D.,‡ SHIRO IRAHA, M.D.,* AKIO HYODO, M.D.,† TAKAFUMI TOITA, M.D.,* YASUMASA KAKINOHANA, PH.D.,* WAKANA TAMAKI, M.D.,* HISAO ITO, M.D.,‖ AND SADAYUKI MURAYAMA, M.D.*

*Department of Radiology, University of the Ryukyus, Okinawa, Japan; †Department of Neurosurgery, University of the Ryukyus, Okinawa, Japan; ‡Department of Radiology, Shinshu University, Fukuoka, Japan; §Department of Radiology, Kyushu University, Nagano, Japan; ‖Department of Radiology, Chiba University, Chiba, Japan; ¶Department of Radiology, Yamanashi University, Yamanashi, Japan; and **Department of Radiology, International Medical Center of Japan, Tokyo, Japan

Purpose: To analyze retrospectively the risk factors of spinal recurrence in patients with intracranial germinoma and clinical outcomes of patients who developed spinal recurrence.

Methods and Materials: Between 1980 and 2007, 165 patients with no evidence of spinal metastases at diagnosis were treated with cranial radiotherapy without spinal irradiation. The median follow-up in all 165 patients was 61.2 months (range, 1.2–260.1 months).

Results: After the initial treatment, 15 patients (9.1%) developed spinal recurrences. Multivariate analysis revealed that large intracranial disease (≥4 cm) and multifocal intracranial disease were independent risk factors for spinal recurrence. Radiation field, total radiation dose, and the use of chemotherapy did not affect the occurrence of spinal recurrences. Of the 15 patients who experienced spinal recurrence, the 3-year actuarial overall survival and disease-free survival (DFS) rates from the beginning of salvage treatments were 65% and 57%, respectively. In the analysis, presence of intracranial recurrence and salvage treatment modality (radiotherapy with chemotherapy vs. radiotherapy alone) had a statistically significant impact on DFS. The 3-year DFS rate in patients with no intracranial recurrence and treated with both spinal radiotherapy and chemotherapy was 100%, whereas only 17% in patients with intracranial recurrence or treated with radiotherapy alone ($p = 0.001$).

Conclusion: Large intracranial disease and multifocal intracranial disease were risk factors for spinal recurrence in patients with intracranial germinoma with no evidence of spinal metastases at diagnosis. For patients who developed spinal recurrence alone, salvage treatment combined with spinal radiotherapy and chemotherapy was effective in controlling the recurrent disease. © **2008 Elsevier Inc.**

Germinomas, Spinal recurrence, Radiation, Chemotherapy.

INTRODUCTION

Intracranial germinomas represent 0.5–2.5% of all intracranial tumors and are more common in Japan than in Western countries (1–5). These tumors occur primarily in the pineal or neurohypophyseal regions and most often affect teenagers and young adults. In contrast to intracranial nongerminomatous germ cell tumors, germinomas are one of the most radiosensitive tumors known and are curable by radiotherapy alone (1, 5–13). Although radiotherapy has been the standard treatment for intracranial germinoma for many years, agreement on the optimal management of these tumors has not been reached. One of the major controversies in the management of intracranial germinoma is the use of craniospinal irradiation in patients with no evidence of spinal metastases at diagnosis (14–18).

Recently, several reports have indicated that the incidence of spinal recurrence was found to be too low to warrant routine spinal irradiation. With modern imaging procedures, the proportion of patients presenting with spinal disease at the time of diagnosis is low, and the risk of secondary spinal seeding in germinoma did not exceed 15% in a large series (8, 19, 20). However, the risk factors for spinal recurrence in patients with no evidence of spinal metastases at diagnosis have not been well documented. Moreover, there is minimal information

Reprint requests to: Dr. Kazuhiko Ogawa, Department of Radiology, Graduate School of Medical Science, University of the Ryukyus, 207 Uehara, Nishihara-cho, Okinawa, 903–0215, Japan. Tel: (+81) 98-895-3331 (ext. 2401); Fax: (+81) 98-895-1420; E-mail: kogawa@med.u-ryukyu.ac.jp

Conflict of interest: none.

Received Jan 17, 2008, and in revised form March 11, 2008. Accepted for publication March 12, 2008.

regarding the outcomes of salvage treatment for patients who developed spinal recurrence. In the current study, we reviewed a retrospective and multi-institutional series of 165 patients with intracranial germinoma who had no evidence of spinal metastases at diagnosis and evaluated the risk factors for spinal recurrence and treatment outcomes for patients who developed spinal recurrences after the initial treatment.

METHODS AND MATERIALS

Patient characteristics

A retrospective review of medical records between 1980 and 2007 identified 240 patients with documented intracranial germinoma treated by radiotherapy at the Department of Radiology, University of the Ryukyus Hospital, Kyushu University Hospital, Shinshu University Hospital, Chiba University Hospital, Yamanashi University Hospital, or the International Medical Center of Japan. Of these, 75 patients having spinal metastases at diagnosis or treated with spinal irradiation were excluded, and a total of 165 patients with no evidence of spinal metastases at diagnosis and treated with cranial radiotherapy without spinal irradiation were subjected to this analysis. With regard to the 75 patients treated with spinal irradiation, 68 patients had no evidence of spinal metastases at diagnosis. The majority of these 68 patients were treated with routine craniospinal irradiation regardless of their disease status between 1980 and 1995, and the disease characteristics of these 68 patients, such as the tumor size and the number of tumor, were not significantly different compared with those of 165 patients treated without spinal irradiation.

Table 1 indicates the patient and treatment characteristics of all 165 patients. All patients were evaluated by computed tomography or magnetic resonance imaging (MRI) scans before initial treatment. One hundred and two patients (62%) were diagnosed pathologically; the remaining 63 patients (38%) were diagnosed clinically as having germinoma by clinical and neuroradiologic signs, as described previously (6, 9, 26). For the assessment of spinal metastases at diagnosis, 81 patients (49%) were evaluated by spinal MRI and the remaining 84 patients were evaluated by cerebrospinal fluid cytology or cerebrospinal fluid tumor markers. Forty patients (24%) had multifocal tumors involving more than one intracranial site, and serum human gonadotropin levels were elevated in 34 (21%) patients, who as a group had a median human gonadotropin value of 44 mIU/mL (range, 15–251 mIU/mL). Patients with human gonadotropin levels greater than 100 mIU/mL had pathologically verified germinomas. No patients had elevated alpha-fetoprotein or carcinoembryonic antigen titer.

Radiotherapy

Details of radiotherapy method were described as previously (21). In brief, radiotherapy was administered using a ^{60}Co teletherapy unit (4 patients), or a 4-, 6-, or 10-MV linear accelerator, and daily fraction sizes of 1.8–2.0 Gy for the primary tumor 5 days per week were mostly used. In most cases, treatment fields were determined using conventional X-ray simulators. For some cases, in an effort to spare normal brain from the high-dose volume of irradiation, computed tomography simulators were also used to boost the primary disease site. Localized-field irradiation was defined as a partial brain field covering the primary tumor with a generous margin, but not including the third ventricle and lateral ventricles.

One hundred three patients (62%) were treated using a radiation field encompassing the whole brain with or without a boost, 42 patients with the whole ventricle with or without a boost, and 20 patients with a localized-field smaller than the whole ventricle (Table 2). The total dose to the primary site ranged from 24 to 59.5 Gy (median, 48.5 Gy), with 7 patients (4%) receiving total doses of >55 Gy because we previously lacked a consensus regarding optimal doses for these tumors, especially for large tumors. Whole-brain doses ranged from 19.5 to 44 Gy (median, 30 Gy), whole-ventricle doses ranged from 24 to 40 Gy (median, 25.2 Gy), and localized-field doses ranged from 24 to 55.8 Gy (median, 40 Gy).

Table 1. Patient and treatment characteristics (n = 165)

Characteristic	No. of patients
Age (median, 17 y)	
<20 y	109 (66)
≥20 y	56 (34)
Gender	
Female	38 (23)
Male	127 (77)
KPS	
≥70	128 (78)
<70	27 (16)
Unknown	10 (6)
Tumor location	
Pineal	65 (39)
Neurohypophyseal	46 (28)
Thalamus or basal ganglia	14 (9)
Multifocal	40 (24)
No. of tumor	
Single	125 (76)
Multifocal	40 (24)
Maximal tumor size (cm)	
<4	131 (79)
≥4	34 (21)
Serum hCG level	
Normal	131 (79)
High	34 (21)
Pathology	
Verified	102 (62)
Unverified	63 (38)
Spinal MRI evaluation at diagnosis	
Yes	81 (49)
No	84 (51)
Total radiation dose (Gy)	
≤50	131 (79)
>50	34 (21)
Treatment field	
WB/WV ± B	145 (88)
Local	20 (12)
Chemotherapy	
Yes	75 (45)
No	90 (55)

Abbreviations: KPS = Karnofsky performance status; hCG = human chorionic gonadotropin; MRI = magnetic resonance imaging; WB/WV = whole brain/whole ventricle; B = boost.

Data in parentheses are percentages.

For patients with spinal recurrences, spinal radiotherapy with or without cranial radiotherapy was administered. The method of spinal radiotherapy was described as previously (22). In brief, spinal irradiation was supplemented using a posteroanterior field with single doses of 1.6–2.0 Gy per fraction and five fractions per week.

Chemotherapy

Seventy-five patients (45%) received systemic chemotherapy with a total of one to six courses (median, three courses) during the initial treatment to reduce the total number of radiation doses

Table 2. Radiation field, total radiation dose, and incidences of intracranial and spinal recurrences according to the treatment modality

Treatment modality	Radiation field	Total radiation dose (range) (Gy)	No. of pts.	No. of low-risk group for SR*	No. of intracranial recurrence	No. of spinal recurrence
RT alone						
	WB ± B	50 (38–59.5)	77	18	1	5
	WV ± B	45 (40–52)	4	0	2	1
	Local	48 (24–55.8)	9	0	3	2
	Total	50 (24–59.5)	90	18 (20%)	6 (7%)	8 (9%)
RT + CT						
	WB ± B	49 (30–55)	26	10	2	4
	WV ± B	30 (24–50)	38	15	1	3
	Local	30 (24–40)	11	0	1	0
	Total	40 (24–50)	75	25 (33%)	4 (5%)	7 (9%)
Total		48.5 (24–59.5)	165	43 (26%)	10 (6%)**	15 (9%)**

Abbreviations: RT = radiotherapy; CT = chemotherapy; WB = whole brain; WV = whole ventricle; B = boost; SR = spinal recurrence; MRI = magnetic resonance imaging.

* Defined as patients with spinal MRI stage negative, small tumor (<4 cm), unifocal tumor, and treatment with WB or WV.

** Four patients developed both intracranial and spinal recurrences.

or radiation fields (Table 2). In patients with radiotherapy alone (median total dose, 50 Gy), 77 of 90 patients (86%) were treated with whole-brain irradiation with or without boost, whereas in patients with radiotherapy and chemotherapy (median total dose, 40 Gy), only 35% of the patients (26 of 75 patients) were treated with whole brain irradiation with or without boost. In the current study, we did not intend to use chemotherapies to reduce the risk of spinal recurrences for these patients. Of 75 patients, 71 patients (95%) received chemotherapy before radiotherapy; 2 patients during radiotherapy and the remaining 2 patients after radiotherapy. All patients received cisplatin or carboplatin in combination with other agents. The most commonly used regimen was a combination of cisplatin and etoposide (35 patients), and the next most common was a combination of carboplatin and etoposide (28 patients). Nine patients received a combination of ifosfamide, cisplatin, and etoposide and 3 patients received a combination of cisplatin and methotrexate. The remaining 1 patient received cisplatin-vinblastine-bleomycin combination therapy. Cycles were usually repeated every 3–4 weeks. Cisplatin and etoposide therapy consisted of cisplatin (20 mg/m^2) and etoposide (60 mg/m^2) for 5 consecutive days (Days 1–5) (23). In the carboplatin and etoposide therapy group, carboplatin (450 mg/m^2) was given on Day 1 and etoposide (150 mg/m^2) was given for 3 consecutive days (Days 1–3) (24). The ifosfamide, cisplatin, and etoposide regimen consisted of iphosphamide (900 mg/m^2), cisplatin (20 mg/m^2), and etoposide (60 mg/m^2) for 5 consecutive days (25); the combination of cisplatin and methotrexate regimen consisted of 50 mg/m^2 of cisplatin on Day 1 with 3 mg of intrathecal methotrexate twice during initial treatment. The cisplatin-vinblastine-bleomycin regimen consisted of cisplatin (20 mg/m^2) for 5 consecutive days (Days 1–5), vinblastine (4–6 mg/m^2) on Days 1 and 8, and bleomycin (10–15 mg/m^2) on Days 1, 8, and 15 (26).

For patients with spinal recurrences, the chemotherapy regimens described here were administered to patients who received both radiotherapy and chemotherapy as a salvage treatment.

Statistical analysis

The median follow-up time of all 165 patients was 61.2 months (range, 1.2–260.1 months), and no patients were lost to follow-up.

Table 3. Clinical data on 15 patients with spinal recurrence (at initial treatment)

Pts. no.	Age	Gender	Pathologic confirmation	Serum hCG	KPS (%)	Primary tumor site	Maximal tumor size (cm)	Total radiation dose	Radiation field	Use of CT	CT regimen (initial Tx)
1	20	Male	Yes	Normal	100	P+N	2	30	WV	Yes	EP
2	15	Male	Yes	Normal	60	P	5	50	WB+L	No	—
3	27	Male	Yes	Elevated	100	P	3	50	WV+L	Yes	CBDCA+VP16
4	27	Male	No	Normal	100	P	2	46	WB+L	No	—
5	12	Female	Yes	Elevated	90	N	4.5	40	WB+L	Yes	EP
6	10	Female	No	Elevated	100	P+N	4	40	L	No	—
7	2	Female	Yes	Normal	40	P	2.5	20	L	No	—
8	17	Female	Yes	Normal	100	N+D	3	40	WB+L	No	—
9	20	Male	Yes	Normal	90	P+N+D	3	50	WB+L	Yes	CBDCA+VP16
10	16	Male	Yes	Normal	100	P	5	50	WB+L	No	—
11	18	Female	No	Normal	100	P	1.5	50	WB+L	No	—
12	30	Male	Yes	Elevated	100	P+D	4.5	50	WV	Yes	CBDCA+VP16
13	13	Male	No	Normal	100	N+D	4	59.5	WB+L	Yes	CDDP+MTX
14	14	Male	No	Normal	90	N+Pons	4.5	48.5	WB+L	Yes	CDDP+MTX
15	14	Male	Yes	Normal	90	P+N	4	50	WV	No	—

Abbreviations: hCG = human chorionic gonadotropin; KPS = Karnofsky performance status; CT = chemotherapy; Tx = therapy; P = pineal; N = neurohypophyseal; D = dissemination; WB = whole brain; WV = whole ventricle; L = local; EP = cisplatin and etoposide; EP = cisplatin and etoposide; CBDCA = carboplatin; VA-16 = etoposide; MTX = methotrexate.

Table 4. Clinical data on 15 patients with spinal recurrence (at spinal recurrence)

Pts. no.	Age at spinal recurrence	Spinal recurrence site	Intracranial recurrence	Spinal radiation field	Spinal radiation dose (Gy)	Intracranial RT	CT after spinal recurrence	CT regimens after spinal recurrence	No. of cycles of CT	Site of re-recurrence after salvage Tx	Outcome	Follow up
1	24	C2-3	No	WS	30.6	No	Yes	ICE	3	—	NED	46.0 Mo
2	18	Th8-9	No	WS+L	45	No	Yes	ICE	4	—	NED	27.7 Mo
3	28	Th4	Yes	WS+L	30.6	Yes (24 Gy)	Yes	ICE	3	Intracranial	Dead	9.8 Mo
4	43	L1-3	No	WS+L	46	No	Yes	ICE	5	—	NED	193.9 Mo
5	18	Multiple	Yes	WS+L	46	Yes (20 Gy)	Yes	EP	3	Intracranial	AWD	69.6 Mo
6	13	Multiple	No	WS	36.3	No	Yes	CBDCA+VP16	3	—	NED	6.3 Mo
7	2	Multiple	Yes	WS	30.6	No	No	-	-	Intracranial, Spinal	Dead	2.1 Mo
8	24	L2	Yes	WS+L	44	Yes (18 Gy)	Yes	CBDCA+VP16	3	Intracranial	AWD	78.0 Mo
9	25	C5-Th2	No	WS+L	45	No	Yes	ICE	3	—	NED	59.4 Mo
10	17	Multiple	No	WS	24	No	No	-	-	Spinal	Dead	10.3 Mo
11	18	Th6-7, L4	No	WS	30	No	Yes	CBDCA+VP16	3	Intracranial	Dead	87.0 Mo
12	30	Multiple	No	WS	30	No	Yes	CBDCA+VP16	3	—	NED	2.8 Mo
13	14	Multiple	No	WS	33	No	Yes	CBDCA+VP16	3	—	NED	5.6 Mo
14	15	Multiple	No	WS	20	No	No	-	-	Spinal	Dead	17.1 Mo
15	15	Th12-S3	No	WS+L	45	No	Yes	CBDCA+VP16	3	—	NED	8.9 Mo

Abbreviations: RT = radiotherapy; CT = chemotherapy; Tx = therapy; C = cervival spine; Th = thoracic spine; L = lumbar spine; WS = whole spine; L = localized field; ICE = ifosphamide, cisplatin, and etoposide; PE = cisplatin and etoposide; CBDCA = carboplatin; VP-16 = etoposide; NED = no evidence of disease; AWD = alive with disease; Mo = months.

For the assessment of risk factors for spinal recurrence, the chi-square test and logistic regression analysis were used to investigate the relationship between variables and the occurrence of spinal recurrence. For the assessment of treatment outcomes for patients who developed spinal recurrence, overall and disease-free survival (DFS) rates were calculated actuarially according to the Kaplan-Meier method (27) and were measured from the beginning of salvage treatment. Differences between groups were estimated using the log–rank test (28). A probability level of 0.05 was chosen for statistical significance, and statistical analysis was performed using the SPSS software package (version 11.0; SPSS, Inc., Chicago, IL).

RESULTS

After the initial treatment, 10 patients (6%) developed intracranial recurrence and 15 patients (9.1%) developed spinal recurrences (Table 2). The median duration from the date of initial treatment to the date of spinal recurrence was 16.8 months (range, 2.4–199.2 months). Patient and disease characteristics in 15 patients with spinal recurrence were listed in Tables 3 and 4.

As shown in Table 5, the incidence of spinal recurrences was significantly higher in patients with primary large (≧4 cm) tumor at initial diagnosis than those without large tumors. Concerning the maximal tumor size, a cutoff size of 4 cm was used because the incidences of spinal recurrence increased as the tumor size increased, especially to 4 cm or larger (Table 6). Also, the incidence of spinal recurrence was significantly higher in patients with primary multifocal tumor at initial diagnosis compared with those without multifocal tumors. No significant differences were seen with respect to other factors, such as radiation field, total radiation dose, and the use of chemotherapy (Table 5). Of these 40 multifocal primary tumors, 18 tumors were bifocal (pineal and neurohypophyseal), and 3 of 18 patients (17%) with these bifocal germinoma had spinal recurrence after the initial treatment. Multivariate analysis revealed that large intracranial disease and multifocal intracranial disease each were independent risk factors for spinal recurrence (Table 5). We were able to define a low-risk group for spinal recurrence as patients with spinal MRI stage negative, small tumor (<4 cm), unifocal tumor, and treatment with whole-brain or whole-ventricle irradiation (Table 2). None of these 43 patients (0%) in the low-risk group developed spinal recurrence, whereas 15 of 122 patients who did not meet the criteria of the low-risk group (12%) developed spinal recurrence.

Regarding the 15 patients who experienced spinal recurrences, the 3-year actuarial overall survival and DFS rates from the beginning of salvage treatments were 65% and 57%, respectively (Fig. 1). The median total dose to the recurrent spinal disease for all 15 patients was 33 Gy (range, 24–46 Gy), and the total doses of salvage cranial radiotherapy for 3 patients ranged from 18 Gy to 24 Gy (Table 4). These 3 patients had intracranial recurrences at lesions initially treated with doses of 20–24 Gy, and the recurrent diseases extended to the margins of initial boost radiation field. In the analysis, the presence of intracranial recurrence and salvage treatment modality (radiotherapy with chemotherapy vs. radiotherapy alone) had a statistically significant

Table 5. Univariate and multivariate analysis of various potential prognostic factors for spinal recurrence in patients with intracranial germinoma

Variable	No. of pts.	No. of spinal recurrence	Univariate *p* value	Multivariate RR (95%C1)	Multivariate *p* value
Tumor size					
<4 cm	131	7 (5%)	< 0.001	0.141 (0.043–0.462)	0.001
≥4 cm	34	8 (24%)			
Tumor number					
Single	125	8 (6%)	0.033	0.230 (0.070–0.761)	0.016
Multifocal	40	7 (18%)			
Gender					
Female	38	5 (13%)	0.320	—	—
Male	127	10 (8%)			
Pathology					
Verified	102	11 (11%)	0.335	—	—
Unverified	63	4 (6%)			
Spinal MRI at diagnosis					
Yes	81	6 (7%)	0.460	—	—
No	84	9 (11%)			
Total radiation dose					
≤50 Gy	131	13 (10%)	0.470	—	—
>50 Gy	34	2 (6%)			
Serum hCG					
Normal	131	11 (8%)	0.542	—	—
High	34	4 (12%)			
KPS					
≥70%	128	13 (10%)	0.660	—	—
<70%	27	2 (7%)			
Unknown	10				
Radiation field					
WB/WV	145	13 (9%)	0.880	—	—
Local	20	2 (10%)			
Age					
<20 y	109	10 (9%)	0.897	—	—
≥20 y	56	5 (9%)			
Use of chemotherapy					
Yes	75	7 (9%)	0.920	—	—
No	90	8 (9%)			

Abbreviations: MRI = magnetic resonance imaging; hCG = human chorionic gonadtropin; KPS = Karnofsky performance status; WB/WV = whole brain/whole ventricle; RR = relative risk; CI = confidence intervals.

impact on DFS (Table 7). All 3 patients treated with spinal radiotherapy alone died of the disease and all 4 patients with intracranial recurrence died of the disease or were alive with the recurrent disease during the period of this analysis.

Concerning intracranial recurrence and treatment modality, we defined the favorable-prognosis group as patients with no intracranial recurrence who were treated with both spinal radiotherapy and chemotherapy, and the unfavorable-prognosis group as patients with intracranial recurrence or those treated with radiotherapy alone. Four of 9 patients from the favorable risk group and 3 of 6 patients from the unfavorable risk group had spinal MRI evaluation at the time of initial diagnosis. The 3-year DFS rate in the favorable prognosis group was 100%, but only 17% in unfavorable prognosis group ($p = 0.001$, Fig. 2). No patients in the favorable risk group developed late complications, such as neurocognitive dysfunctions, vascular pathology, or leukoencephalopathy after salvage treatments.

Table 6. Incidences of spinal recurrence according to the maximal tumor size

Maximal tumor size	No. of pts.	No. of pts. with spinal recurrence
<2 cm	35	1 (3%)
≤2 cm <4 cm	96	6 (6%)
≥4 cm	34	8 (24%)
Total	165	15 (9%)

DISCUSSION

The current study indicated that large intracranial disease and multifocal intracranial disease at initial diagnosis were independent risk factors for spinal recurrence in patients with intracranial germinoma with no evidence of spinal metastases at diagnosis. Concerning the primary tumor size, several reports have indicated that tumor size is an independent prognostic factor for these tumors (6, 29, 30). Shibamoto *et al.* indicated that a tumor size <3 cm was associated with a better prognosis in patients with intracranial germinoma

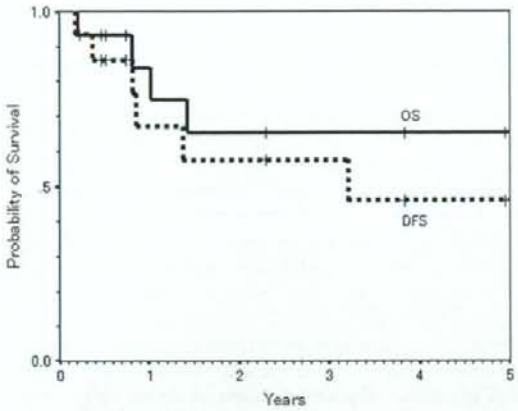

Fig. 1. Actuarial overall survival (OS) and disease-free survival (DFS) for all 15 patients with intracranial germinoma who developed spinal recurrence from the beginning of salvage treatment.

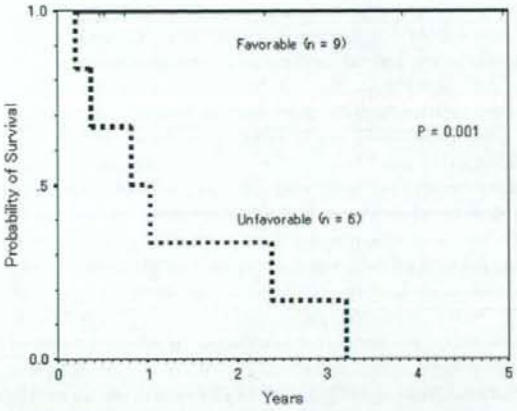

Fig. 2. Actuarial disease-free survival rates from the beginning of salvage treatment according to the presence of intracranial recurrence and treatment modality in patients with intracranial germinoma who developed spinal recurrences.

(30). Shirato *et al.* treated 51 patients with intracranial germinoma, and of 4 patients with more than 4-cm tumor, 1 patient (25%) had a spinal recurrence (6). In the current study, the incidence of spinal recurrence was significantly higher in patients with intracranially large tumor than those without large tumors, and large primary tumor was found to be an independent risk factor for spinal recurrence. These results suggest that craniospinal irradiation appears to be appropriate in patients with large primary tumors, even if there is no evidence of spinal metastases at diagnosis.

Table 7. Univariate analysis of various potential prognostic factors for disease-free survival in patients with intracranial germinoma who developed spinal recurrence

Variable	No. of pts.	3-year DFS (%)	*p* Value
Salvage treatment modality			
RT and CT	12	76	0.002
RT alone	3	0	
Presence of intracranial recurrence			
Yes	4	0	0.018
No	11	71	
Age			
<20 y	10	40	0.127
≥20 y	5	75	
Spinal radiation dose			
<40 Gy	9	38	0.163
≥40 Gy	6	75	
Pathology			
Verified	10	49	0.370
Unverified	5	67	
KPS			
≥70%	13	57	0.378
<70%	2	0	
Initial serum hCG level			
Normal	11	65	0.437
High	4	38	

Abbreviations: RT = radiotherapy; CT = chemotherapy; KPS = Karnofsky performance status; hCG = human chorionic gonadotropin; DFS = disease-free survival.

Concerning the number of primary tumors, several authors have recommended craniospinal irradiation for multifocal tumors (19, 31). Lindstadt *et al.* recommended that patients with documented subependymal or subarachnoid metastases presumably are at higher risk for leptomeningeal failure and recommended craniospinal irradiation for these patients (19). Dalttoli *et al.* advocated that craniospinal irradiation should be administered to patients with disease involving more than one intracranial site, demonstrated meningeal seeding, or positive cerebrospinal fluid cytology (31). In the current study, the incidence of spinal recurrence was significantly higher in patients with intracranially multifocal tumor at initial diagnosis than those without intracranially multifocal tumors. Moreover, the multivariate analysis revealed that multifocal primary tumor was found to be an independent risk factor for spinal recurrence. These results suggest that craniospinal irradiation appears to be appropriate in patients with multifocal tumors even if there is no evidence of spinal dissemination at the time of initial diagnosis.

However, optimal management of primary intracranial pineal and neurohypophyseal (bifocal) germinomas still remains controversial (3, 32, 33). Shibamoto *et al.* advocated that when the disease extends along the ventricular walls or is present in both pineal and neurohypophyseal regions, craniospinal irradiation should be considered, taking the patient's age into account (3). Conversely, Lafay-Cousin *et al.* suggested that bifocal germinoma can be considered a locoregional rather than a metastatic disease (33). The definition as either located or disseminated diseases has major implications on required treatment and its associated late morbidity. Moreover, the pathogenesis of such bifocal lesion is contested and the optimal management remains controversial. In the current study, 3 of 18 patients (17%) with bifocal germinoma had spinal recurrences. From our results, bifocal germinoma may

have some potential to metastasize and we advocate that patients with bifocal germinoma should be treated with craniospinal irradiation, taking the patient's age into account.

Although the optimal radiotherapy dose to the primary tumor is still unclear, recent findings have suggested that intracranial germinomas can be generally be cured with doses of between 40 and 50 Gy (3, 5, 6, 9, 20). In the current study, doses greater than 50 Gy were not associated with a decreased risk of spinal recurrence (Table 5). Therefore, doses of 40–50 Gy appear to be appropriate for the primary tumor. Concerning the optimal radiation dose required for the control of microscopic disease, most authors have recommended doses of 25–30 Gy for microscopic disease (7, 10, 13, 34). In the current study, we found that intracranial recurrences occurred with lesions treated at doses of 20–24 Gy in 3 patients, and that total doses of 24 Gy or less may be insufficient for microscopic diseases. Recently, Shibamoto *et al.* recommended a lower craniospinal dose of 20–24 Gy, because similar results were obtained for patient groups with positive or negative cytology (20). Schoenfeld *et al.* indicated that radiotherapy alone with low-dose prophylactic craniospinal irradiation (usually 21 Gy at 1.5 Gy per fraction) cured almost all patients with localized intracranial germinoma with rare complications (17). Further studies are needed to determine whether even lower doses can suffice for the control of microscopic disease.

Recently, to reduce the total radiation doses, the combination of chemotherapy and low-dose radiotherapy has being increasingly investigated (25, 26). The approach of delivering reduced-dose limited-field radiotherapy after a complete response to chemotherapy appears to be meritorious. However, our results indicated that chemotherapy was not associated with decreased risk of spinal recurrences (Table 5). Therefore chemotherapy alone appears to be insufficient to eradicate the microscopic spinal diseases, and spinal radiotherapy is recommended as a prophylactic treatment for spinal recurrence.

Concerning the treatment results for spinal recurrence, our results indicated that presence of intracranial recurrence and treatment modality (radiotherapy with chemotherapy vs. radiotherapy alone) each had a statistically significant impact on DFS. In particular, considering both the presence of intracranial recurrence and the treatment modality, the 3-year DFS in patients with no intracranial recurrence and treated with radiotherapy and chemotherapy was 100%, whereas only 17% in patients with intracranial recurrence and/or treated with radiotherapy alone ($p = 0.001$). Although there have been few reports describing the treatment results of spinal recurrences from intracranial germinoma, recent reports with unusual cases have indicated the efficacy of radiotherapy combined with chemotherapy for spinal tumors (35, 36). Merchant *et al.* treated 8 patients with intracranial germinoma who relapsed after treatment with primary chemotherapy. Of these 8 patients, 2 had spinal recurrences (tumor cells detected by MRI or cytologic evidence of cerebrospinal fluid involvement) and both were successfully treated with combination chemotherapy and radiotherapy (35). Tosaka *et al.* experienced a patient with spinal recurrence from intracranial germinoma who was successfully treated with 24 Gy spinal radiotherapy and several courses of systemic chemotherapy containing carboplatin, etoposide, and iphosphamide, with no recurrences after 1 year (36). Our results indicated that 3-year DFS in patients treated with radiotherapy and chemotherapy was significantly higher than that in patients treated with radiotherapy alone ($p = 0.002$). These results indicated that in patients with spinal recurrence alone, radiotherapy with chemotherapy was effective in controlling the recurrent diseases and should be recommended as a salvage treatment for these recurrent tumors.

Conversely, our results indicated that the patients with intracranial recurrences or treated with radiotherapy alone had a poor prognosis. For patients with intracranial recurrence, most patients have already received approximately 30–50 Gy to the brain and only insufficient radiation doses can be applied to the recurrent intracranial disease. In the current study, total doses of salvage cranial radiotherapy for 3 patients with intracranial recurrence were 18–24 Gy, which appeared to be insufficient for controlling the recurrent intracranial diseases, and all 3 patients were dead or alive with recurrent disease despite salvage therapies. Therefore, from our results, the optimal initial treatment at diagnosis is necessary to reduce the risk of intracranial recurrence (37–39). Concerning treatment modalities, our results indicated that 3 patients treated with spinal radiotherapy alone all died of the disease. Therefore spinal radiotherapy alone appears to be insufficient to control the recurrent spinal diseases.

In conclusion, our results indicated that large intracranial tumor and multifocal intracranial tumor were independent risk factors for spinal recurrence in patients with intracranial germinoma with no evidence of spinal metastases at initial diagnosis, and craniospinal irradiation appears to be appropriate for these patients. Our results also indicated that for patients who developed spinal recurrences alone, a combination of radiotherapy and chemotherapy was effective in controlling recurrent spinal diseases, and should be recommended as a salvage treatment for these recurrent tumors. However, this study is a retrospective study with a various treatment regimens, and further prospective studies are required to confirm our results.

REFERENCES

1. Bamberg M, Kortmann RD, Calaminus G, *et al.* Radiation therapy for intracranial germinoma: Results of the German cooperative prospective trials MAKEI 83/86/89. *J Clin Oncol* 1999;17: 2585–2592.
2. Sutton LN, Radcliffe J, Goldwein JW, *et al.* Quality of life of adult survivors of germinomas treated with craniospinal irradiation. *Neurosurgery* 1999;45:1292–1297.
3. Shibamoto Y, Abe M, Yamashita J, *et al.* Treatment results of intracranial germinoma as a function of the irradiated volume. *Int J Radiat Oncol Biol Phys* 1988;15: 285–290.
4. Aoyama H, Shirato H, Kakuto Y, *et al.* Pathologically-proven intracranial germinoma treated with radiation therapy. *Radiother Oncol* 1998;47:201–205.

5. Hardenbergh PH, Golden J, Billet A, *et al.* Intracranial germinoma: The case for lower dose radiation therapy. *Int J Radiat Oncol Biol Phys* 1997;39:419–426.
6. Shirato H, Nishio M, Sawamura Y, *et al.* Analysis of long-term treatment of intracranial germinoma. *Int J Radiat Oncol Biol Phys* 1997;37:511–515.
7. Brandes AA, Pasetto LM, Monfardini S. The treatment of cranial germ cell tumors. *Cancer Treat Rev* 2000;26:233–242.
8. Matsutani M, Sano K, Takakura K, *et al.* Primary intracranial germ cell tumors: A clinical analysis of 153 histologically verified cases. *J Neurosurg* 1997;86:446–455.
9. Shibamoto Y, Sasai K, Oya N, *et al.* Intracranial germinoma: Radiation therapy with tumor volume-based dose selection. *Radiology* 2001;218:452–456.
10. Haddock MG, Schild SE, Scheithauer BW, *et al.* Radiation therapy for histologically confirmed primary central nervous system germinoma. *Int J Radiat Oncol Biol Phys* 1997;38:915–923.
11. Ogawa K, Toita T, Nakamura K, *et al.* Treatment and prognosis of intracranial non-germinomatous malignant germ cell tumors: A multi-institutional retrospective analysis of 41 patients. *Cancer* 2003;98:369–376.
12. Paulino AC, Wen BC, Mohideen MN. Controversies in the management of intracranial germinomas. *Oncology (Williston Park)* 1999;13:513–521.
13. Fields JN, Fulling KH, Thomas PR, *et al.* Suprasellar germinoma: Radiation therapy. *Radiology* 1987;164:247–249.
14. Rogers SJ, Mosleh-Shirazi MA, Saran FH. Radiotherapy for localized intracranial germinoma: Time to sever historical ties? *Lancet Oncol* 2005;6:509–519.
15. Maity A, Shu HK, Janss A, *et al.* Craniospinal radiation in the treatment of biopsy-proven intracranial germinomas: Twenty-five years' experience in a single center. *Int J Radiat Oncol Biol Phys* 2004;58:1165–1170.
16. Merchant TE, Sherwood SH, Mulhern RK, *et al.* CNS germinoma: Disease control and long-term functional outcome for 12 children treated with craniospinal irradiation. *Int J Radiat Oncol Biol Phys* 2000;46:1171–1176.
17. Schoenfeld GO, Amdur RJ, Schmalfuss IM, *et al.* Low-dose prophylactic craniospinal radiotherapy for intracranial germinoma. *Int J Radiat Oncol Biol Phys* 2006;65:481–485.
18. Nguyen QN, Chang EL, Allen PK, *et al.* Focal and craniospinal irradiation for patients with intracranial germinoma and patterns of failure. *Cancer* 2006;107:2228–2236.
19. Linstadt D, Wara WM, Edwards MS, *et al.* Radiotherapy of primary intracranial germinomas: The case against routine craniospinal irradiation. *Int J Radiat Oncol Biol Phys* 1988;15: 291–297.
20. Ogawa K, Shikama N, Toita T, *et al.* Long-term radiotherapy for intracranial germinoma: A multi-institutional retrospective review of 126 patients. *Int J Radiat Oncol Biol Phys* 2004;58: 705–713.
21. Ogawa K, Toita T, Kakinohana Y, *et al.* Radiation therapy for intracranial germ cell tumors: Predictive value of tumor response as evaluated by computed tomography. *Int J Clin Oncol* 1997;2:67–72.
22. Shikama N, Ogawa K, Tanaka S, *et al.* Lack of benefit of spinal irradiation in the primary treatment of intracranial germinoma: A multiinstitutional, retrospective review of 180 patients. *Cancer* 2005;104:126–134.
23. Yoshida J, Sugita K, Kobayashi T, *et al.* Prognosis of intracranial germ cell tumours: Effectiveness of chemotherapy with cisplatin and etoposide (CDDP and VP-16). *Acta Neurochir (Wien)* 1993;120:111–117.
24. Matsutani M, Sano K, Takakura K, *et al.* Combined treatment with chemotherapy and radiation therapy for intracranial germ cell tumors. *Child Nerv Syst* 1998;14:59–62.
25. Aoyama H, Shirato H, Ikeda J, *et al.* Induction chemotherapy followed by low-dose involved-field radiotherapy for intracranial germ cell tumors. *J Clin Oncol* 2002;20:857–865.
26. Matsutani M. The Japanese Pediatric Brain Tumor Study Group. Combined chemotherapy and radiation therapy for CNS germ cell tumors—the Japanese experience. *J Neurooncol* 2001;54:311–316.
27. Kaplan EL, Meier P. Nonparametric estimation from incomplete observations. *J Am Stat Assoc* 1958;53:457–481.
28. Mantel N. Evaluation of survival data and two new rank order statistics arising in its consideration. *Cancer Chemother Rep* 1966;50:163–170.
29. Sung DI, Harisliadis L, Chang CH. Midline pineal tumors and suprasellar germinomas: Highly curable by irradiation. *Radiology* 1978;128:745–751.
30. Shibamoto Y, Yakahashi M, Abe M. Reduction of the radiation dose for intracranial germinoma: A prospective study. *Br J Cancer* 1994;70:984–989.
31. Dattoli MJ, Newall J. Radiation therapy for intracranial germinoma: The case for limited volume treatment. *Int J Radiat Oncol Biol Phys* 1990;19:429–433.
32. Lee L, Saran F, Hargrave D, *et al.* Germinoma with synchronous lesions in the pineal and suprasellar regions. *Child Nerv Syst* 2006;22:1513–1518.
33. Lafay-Cousin L, Millar BA, Mabbott D, *et al.* Limited-field radiation for bifocal germinoma. *Int J Radiat Oncol Biol Phys* 2006;65:486–492.
34. Packer RJ, Cohen BH, Cooney K. Intracranial germ cell tumors. *Ongologist* 2000;5:312–320.
35. Merchant TE, Davis BJ, Sheldon JM, *et al.* Radiation therapy for relapsed CNS germinoma after primary chemotherapy. *J Clin Oncol* 1998;16:204–209.
36. Tosaka M, Ogimi T, Itoh J, *et al.* Spinal epidural metastasis from pineal germinoma. *Acta Neurochir (Wien)* 2003;145: 407–410.
37. Osuka S, Tsuboi K, Takano S, *et al.* Long-term outcome of patients with intracranial germinoma. *J Neurooncol* 2007;83:71–79.
38. Nakamura H, Takeshima H, Makino K, *et al.* Recurrent intracranial germinoma outside the initial radiation field: A single-institution study. *Acta Oncol* 2006;45:476–483.
39. Shirato H, Aoyama H, Ikeda J, *et al.* Impact of margin for treatment volume in low-dose involved field radiotherapy after induction chemotherapy for intracranial germinoma. *Int J Radiat Oncol Biol Phys* 2004;60:214–217.

Analytical Biochemistry 383 (2008) 151–158

Contents lists available at ScienceDirect

Analytical Biochemistry

journal homepage: www.elsevier.com/locate/yabio

In-gel multiple displacement amplification of long DNA fragments diluted to the single molecule level

Yuichi Michikawa [a], Keisuke Sugahara [a,b], Tomo Suga [a], Yoshimi Ohtsuka [a], Kenichi Ishikawa [a], Atsuko Ishikawa [a], Naoko Shiomi [a], Tadahiro Shiomi [a], Mayumi Iwakawa [a], Takashi Imai [a,*]

[a] RadGenomics Project, Research Center for Charged Particle Therapy, National Institute of Radiological Sciences, Inage, Chiba 263-8555, Japan
[b] Department of Oral and Maxillofacial Surgery, Tokyo Dental College, Mihama, Chiba 261-8502, Japan

ARTICLE INFO

Article history:
Received 28 April 2008
Available online 20 August 2008

Keywords:
Multiple displacement amplification
Alkaline agarose gel
Phi29 DNA polymerase
Haplotype
Homologous chromosome

ABSTRACT

The isolation and multiple genotyping of long individual DNA fragments are needed to obtain haplotype information for diploid organisms. Limiting dilution of sample DNA followed by multiple displacement amplification is a useful technique but is restricted to short (<5 kb) DNA fragments. In the current study, a novel modification was applied to overcome these problems. A limited amount of cellular DNA was carefully released from intact cells into a mildly heated alkaline agarose solution and mixed thoroughly. The solution was then gently aliquoted and allowed to solidify while maintaining the integrity of the diluted DNA. Exogenously provided Phi29 DNA polymerase was used to perform consistent genomic amplification with random hexameric oligonucleotides within the agarose gels. Simple heat melting of the gel allowed recovery of the amplified materials in a solution of the polymerase chain reaction (PCR)-ready form. The haplotypes of seven SNPs spanning 240 kb of the DNA surrounding the human ATM gene region on chromosome 11 were determined for 10 individuals, demonstrating the feasibility of this new method.

Single DNA molecule analysis has undergone several innovations directed at solving different biological problems. In general, these methods involve PCR of single copy genes in sperm [1], digital PCR [2], somatic mutations [3], massively parallel sequencing [4], screening of protein expression libraries [5], and analysis of methylation status [6]. These methods have been applied to relatively short target DNA (up to several hundred base pairs) due to the limitations of the polymerase chain reaction (PCR).[1]

Haplotype analysis requires single DNA molecules of greater length (usually >20 kb). A haplotype (haploid genotype) is a set of structurally continuous genetic markers on an individual chromosome [7]. In genetic association studies, identification of a haplotype may facilitate more precise mapping of a target gene within a chromosomal region initially identified by linkage analysis with conventional genetic markers such as single nucleotide polymorphisms (SNPs) and microsatellites [8]. The assessment of haplotypes is also important for more extensive functional studies because genetic markers on the same chromosome may interact functionally with each other [9].

The difficulties associated with the experimental determination of haplotypes, owing to the presence of two nearly identical chromosome copies in diploid cells, have prevented their general use. Haplotypes that span long distances or comprise many genetic markers are difficult to determine experimentally. Currently, most haplotypes are reconstructed indirectly through statistical analyses of conventional genotype data [10] or by inference from familial data [11]. The reliability of statistical estimates depends on various factors such as the number of genetic markers, the population size, the allele frequencies, and the linkage disequilibrium between the genetic markers [12]. Inferences drawn from familial data may be limited by the availability of DNA samples.

Recently, several new molecular haplotyping techniques have been developed (reviewed in Ref. [13]). In particular, the polony approach, which involves PCR amplification by exogenously added *Taq* DNA polymerase of a single copy of the target locus within a polyacrylamide gel followed by in-gel sequential fluorescent single base extension, has proven to be effective for molecular haplotyping at the whole chromosome level [14]. Immobilization of the template DNA within a polyacrylamide gel matrix has the advantage of ensuring spatial separation of the chromosomes while maintaining their structural integrity. However, when the amplified products are to be subjected to further analysis, recovery of DNA fragments after amplification is problematic if the DNA has been immobilized. Thus, this methodology is limited with respect to the number of SNP loci that can be analyzed.

* Corresponding author. Fax: +81 43 2064648.
E-mail address: imait@nirs.go.jp (T. Imai).

[1] *Abbreviations used:* PCR, polymerase chain reaction; SNP, single nucleotide polymorphism; EBV, Epstein–Barr virus; PBS, phosphate-buffered saline; dNTP, deoxynucleoside triphosphate; CP, crossing point; sdH_2O, sterile deionized water; igMDA, in-gel multiple displacement amplification; qPCR, quantitative PCR.

0003-2697/$ - see front matter © 2008 Elsevier Inc. All rights reserved.
doi:10.1016/j.ab.2008.08.011

Other haplotyping approaches have used genomic preamplification of limiting dilutions of sample DNA followed by locus-specific PCR [15,16]. Konfortov and coworkers [15] used PCR-based primer extension preamplification (PEP) [17], in contrast to Paul and Apgar [16], who used multiple displacement amplification (MDA) with Phi29 DNA polymerase [18]. PCR-based PEP is often limited by target length [19–21] and genomic representation [22], although Konfortov and coworkers showed efficient multilocus haplotyping by the TILLING of short DNA fragments [15]. MDA is considered to be more efficient and to provide superior genomic coverage [23,24], so it has become widely used for various purposes. In addition, MDA has a relatively low sequence error rate [24]. Although Paul and Apgar elucidated only the haploid state of the major histocompatibility complex on chromosome 6 [16], MDA should be applicable for further multilocus haplotyping.

During the initial phase of the current study, we experienced serious problems in applying the conditions described by Paul and Apgar [16]. The technique of limiting dilution of sample DNA followed by MDA has been restricted to short (<5 kb) DNA fragments, as demonstrated by the cell-free cloning of amplicons [25]. This restriction may be attributed to cleavage and aggregation problems during the dilution process. Irreversible adsorption of diluted sample DNA to the reaction tubes may also generate experimental inconsistencies.

In the current study, we established that embedding diluted DNA within an agarose gel supports effective genomic preamplification by MDA, thereby facilitating long-range multilocus haplotyping. Agarose gels are used to retain high-molecular-weight DNA in a stable form that is accessible to restriction endonucleases, DNA ligases, and proteinases [26–31]. Because Phi29 DNA polymerase operates at a relatively low temperature, the gel need not be subjected to temperatures above the melting point, meaning that sample integrity is maintained throughout the reaction. Furthermore, the amplified products can easily be recovered in solution from agarose gels by simple heating, making them available for use as templates in further conventional PCR analysis. Using this amplification method in combination with the previously established visible multiple SNP typing array system [32–34], we determined the diplotypes of the human *ATM* locus.

Materials and methods

Materials

Human genomic DNA samples were extracted from blood samples donated by 100 healthy volunteers in a previous study [35]. All donors gave written informed consent to participate in this study, which was approved by the ethics committee at the National Institute of Radiological Sciences (Chiba, Japan). Epstein–Barr virus (EBV)-transformed human lymphoblastoid cell lines were established from the peripheral blood cells of healthy volunteers in a previous study [36]. These cell lines were grown in RPMI 1640 medium (Sigma–Aldrich, Irvine, Ayrshire, UK) that was supplemented with 20% fetal bovine serum (Biological Industries, Kibbutz Beit Haemek, Israel). The cells were washed once with phosphate-buffered saline (PBS) and counted. The cell concentration was adjusted to 5000 cells/ml, and 10-μl aliquots (50 cells) were transferred to new 0.5-ml Eppendorf tubes and stored at −80 °C until use. The oligonucleotides were purchased from Integrated DNA Technologies (IDT, Coralville, IA, USA).

Real-time quantitative PCR

The reaction mixtures (10 μl) contained 0.5 U HotStar *Taq* DNA polymerase (Qiagen, Valencia, CA, USA), 1× HotStar *Taq* DNA polymerase buffer, 0.2 mM deoxynucleoside triphosphates (dNTPs), 3.3× SYBR Green I, 0.2 μM of each PCR primer, and 4 μl of template DNA. The mixtures were heated at 95 °C for 15 min and then subjected to 50 cycles of 95 °C for 10 s and 65 °C for 40 s, followed by melting curve analysis from 65 to 95 °C with a ramp rate of 4.8 °C/s in a LightCycler 480 thermal cycler (Roche Diagnostics, Basel, Switzerland). The crossing point (CP) of each amplification curve was determined by the maximum second derivative method.

Embedding human genomic DNA in an agarose gel

Type I agarose (Sigma–Aldrich) was suspended at 3.75 g per 100 ml of sterile deionized water (sdH_2O), thoroughly heated in a microwave oven, and then allowed to cool down slowly to 60 °C in a heating block. The 3% alkaline agarose was prepared by mixing 960 μl of the agarose solution with 240 μl of a prewarmed alkaline solution (0.5 N NaOH and 1.5 M NaCl), and this solution was maintained at 60 °C. The 3% alkaline agarose solution was mixed with an appropriate amount of human genomic DNA and incubated at 60 °C for 30 min with occasional gentle inversion. Finally, 20-μl aliquots of the mixture were transferred to new 1.5-ml Eppendorf tubes, left at room temperature for 5 min, and then cooled on ice for 5 min.

Embedding lymphoblastoid cell line-derived chromosomal DNA in an agarose gel

Frozen human lymphoblastoid cell lines were thawed at room temperature. Cell suspensions that contained an appropriate number of cells (10 cells in 2 μl) were gently added to 1-ml aliquots of 3% alkaline agarose and incubated at 60 °C for 30 min with occasional gentle inversions. Next, 5-μl aliquots were transferred to new 1.2-ml microtubes (ABgene, Surrey, UK), incubated at room temperature for 5 min, and then cooled on ice for 5 min.

In-gel multiple displacement amplification

Solidified aliquots of gel were washed at room temperature for 10 min with 200 μl of neutralizing solution (0.5 M Tris–HCl [pH 7.4] and 3 M NaCl), followed by washes with 200 μl of 0.5× SSC solution (75 mM NaCl and 7.5 mM sodium citrate [pH 7.0]) for at least 10 min. The gels were then soaked in two-time volume (40 μl for 20-μl gel and 10 μl for 5-μl gel) of in-gel multiple displacement amplification (igMDA) solution that contained 0.75 U/μl Phi29 DNA polymerase (New England Biolabs, Ipswich, MA, USA), 1× Phi29 DNA polymerase buffer, 50 μM random hexamers with phosphorothioate modifications of two consecutive nucleotides at the 3′ end [16], 1.25 mM dNTPs, 1% Tween 20, and 0.1 mg/ml bovine serum albumin. The gels were incubated in a BioShaker (TAITEC, Saitama, Japan) at 30 °C for the indicated time period with constant shaking at 200 rpm. After incubation, the gels were supplemented with sdH_2O to a final volume of 500 μl and were immediately heated at 100 °C for 10 min to terminate the reaction and melt the gels.

Assessment of igMDA amplification

The standard curve method of real-time quantitative PCR (qPCR) was used to determine the concentration of target locus DNA in each amplified DNA sample relative to the concentration of unamplified original DNA, as described by Dean and coworkers [18] with some modifications. A standard curve for each primer pair was generated from the CP at 0, 0.5, 1, 5, and 10 ng of the unamplified original DNA. Next, the amplification yield at each locus was calculated as follows:

yield = target locus DNA amount in 4 μl of post-igMDA solution × total volume of post-igMDA solution/ 4 μl.

The fold amplification of each locus was calculated using the following equation:

fold amplification = amplification yield of target locus/amount of input DNA.

Visible multiple SNP genotyping

A visible, multiple genotyping array for SNPs of the *ATM* gene locus on chromosome 11 was constructed and used as described previously [32–34]. The products of the real-time qPCR obtained in the second screen (see below) were used as templates for SNP genotyping.

MassARRAY SNP typing and haplotype estimation

Typing of the seven SNPs of the *ATM* region was carried out with genomic DNA extracted from 100 healthy volunteers using the MassARRAY system (Sequenom, San Diego, CA) [37] according to the manufacturer's instructions. The haplotypes of the seven SNPs were estimated using the expectation maximization algorithm [10].

Results

Long-range single DNA molecule genotyping

An overview of the entire procedure is shown in Fig. 1. Briefly, cellular DNA was carefully released from intact cells into a mildly heated alkaline agarose solution and mixed thoroughly. The mixture was then carefully aliquoted into new microtubes and solidified by cooling, so that physical separation of embedded homologous chromosome DNA fragments was achieved. After neutralization of the gels, exogenously provided Phi29 DNA polymerase with random hexameric oligonucleotides gave consistent igMDA at 30 °C while maintaining the integrity of the gels throughout the reaction. The heating of the gels after the addition of the aqueous solution terminated the reaction and allowed recovery of the amplified materials, which were suitable for PCR-mediated target locus screening and multiple loci genotyping.

Qualitative assessment of igMDA for different chromosomal loci

Real-time qPCR of various chromosomal loci was used to assess qualitatively the amounts of DNA within the agarose gel after genomic amplification. Three nuclear chromosomal loci (*Securin* gene locus on chromosome 5, *ATM* gene locus on chromosome 11, and *DNA ligase III* gene locus on chromosome 17) and one mitochondrial DNA locus were selected for this purpose. All four loci were successfully amplified (Fig. 2). More than 10 cycle shifts were observed at the CP of the amplification curve for all of the primer sets when a constant amount of heat-melted agarose gel containing amplified genomic DNA was used as the PCR template. These observations confirm that extensive template DNA replication primed by randomly hybridized hexameric oligonucleotides is promoted by the exogenously supplied Phi29 DNA polymerase.

Quantitative assessment of igMDA

The amplification yield for each locus was calculated from the various amounts of input DNA, as described in Materials and Methods (plotted in Supplementary Figs. 1a, 1c, 1e, and 1g in the supplementary material). For the nuclear chromosomal loci, the yields were moderately proportional to the amount of input DNA, although the yield varied among the different loci. The yield of the mitochondrial locus was relatively constant regardless of the amount of input DNA. These differences may reflect differences in amplification kinetics between linear and circular template DNA [38] captured within the limited space of an agarose gel.

The fold amplification of each locus (Supplementary Figs. 1b, 1d, 1f, and 1h) showed a moderate inverse relationship to the amount of input DNA, as reported previously for MDA in solution [18]. A decrease in the amount of input DNA led to a clear increase in amplification, with up to 120,000-fold amplification being achieved and circular mitochondrial DNA showing the steepest increase. These observations indicate that the crowded-

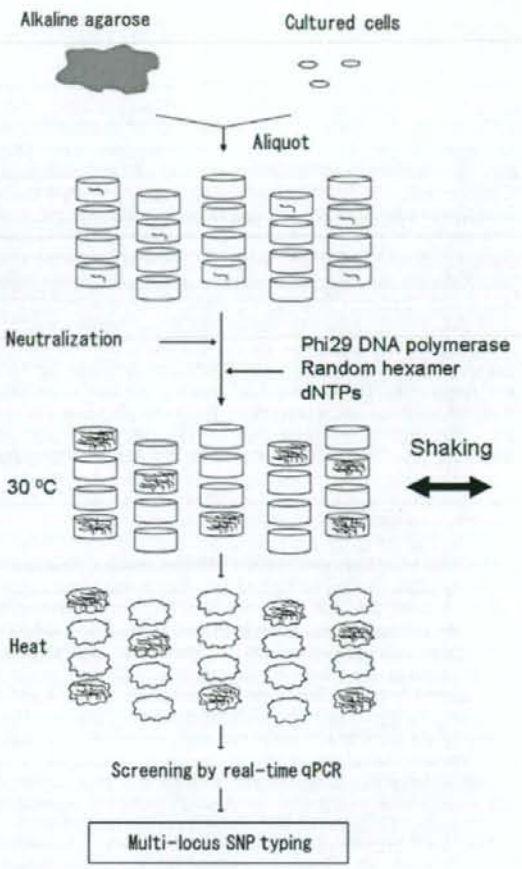

Fig. 1. Outline of the molecular haplotyping experiments. Intact cultured cells were mixed with a heated alkaline agarose gel solution, and small aliquots of the gel were prepared. The gel aliquots were allowed to cool until they solidified and were then neutralized. A reaction mixture that contained Phi29 DNA polymerase, random hexamers, and dNTPs was added to each gel, and the gels were incubated at 30 °C for 16 h. The gels were then heated to terminate the reaction and solubilize the gels. Gels that contained the target chromosome were screened by real-time qPCR and subjected to multilocus genotyping.

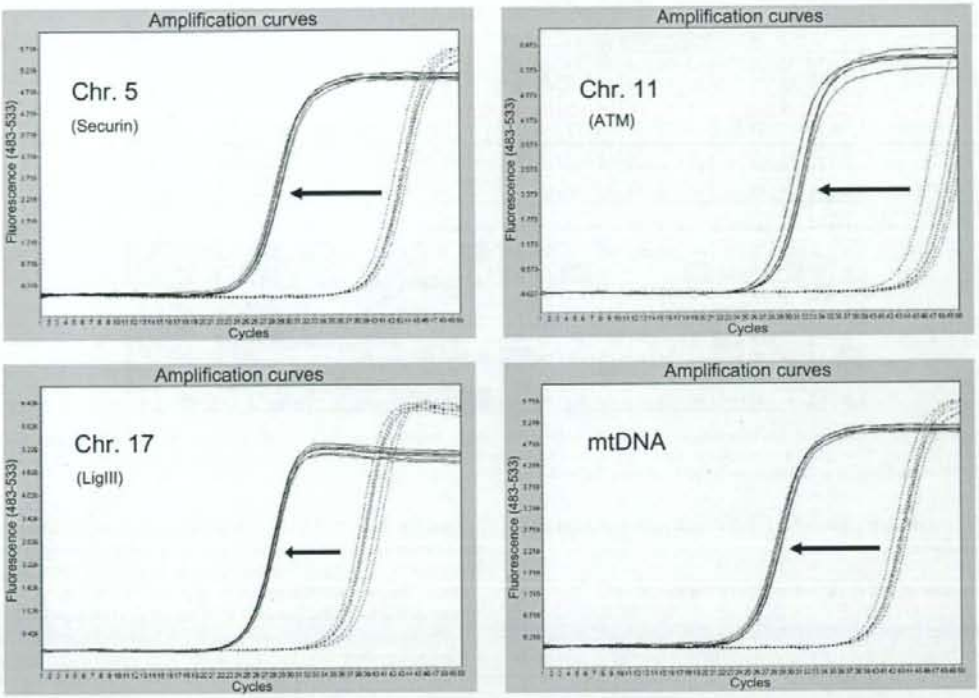

Fig. 2. Real-time qPCR of samples in a heat-solubilized agarose gel. Agarose gels that contained 1 ng of human genomic DNA were incubated either with or without Phi29 DNA polymerase for 16 h. After incubation, sdH_2O was added to the gels to prepare a 100-fold dilution, which was then heat solubilized. Aliquots (4 μl) of the solubilized agarose were used as templates for real-time qPCR. Gels were prepared in duplicate. Real-time qPCR was performed in triplicate for each gel. Solid line: with Phi29 DNA polymerase; broken line: without Phi29 DNA polymerase. Chr., chromosome; LigIII, DNA ligase III; mtDNA, mitochondial DNA. The PCR primers used for each locus are listed in Supplementary Table 1.

ness of template DNA embedded within the agarose gel acts as a rate-limiting factor, especially for circular DNA.

Time course analysis of igMDA

The time course changes in amplification yield from igMDA are shown in Supplementary Fig. 2. The reaction reached a plateau phase after 4–6 h, as reported previously for MDA performed in solution [18]. Constant shaking (solid line in the figure) of the reaction mixture during incubation seemed to improve the amplification balance for all four loci as compared with the nonshaken reaction (broken line).

Embedding cellular DNA molecules in an agarose gel

This experimental system was applied to an EBV-transformed human lymphoblastoid cell line derived from a healthy volunteer [36]. Here 10 cells were mixed with 1 ml of alkaline agarose solution and incubated at 60 °C for 30 min. Next, 5 μl of the solution, containing on average 0.05 cells (0.2 copies of single-stranded chromosomes per aliquot), were aliquoted 93 times from the mix. In addition, two 5-μl aliquots of the gel containing 100 times as many cells (5 cells, average of 20 copies of single-stranded chromosomes per aliquot) and one 5-μl aliquot of gel containing no cells were prepared as positive and negative controls, respectively. All of these gels were subjected to igMDA at 30 °C with constant shaking for 16 h.

First screening of target locus amplicons

The 96 gel samples subjected to igMDA were screened for four target loci (Fig. 3) using real-time qPCR with primer sets designed to amplify each target locus and the heat-melted gel portions as templates. The numbers of gels that were positive for each locus were 7, 9, 10, and 71, respectively, and all included the two positive control gels. Gel samples that were positive for the three nuclear chromosomal loci appeared at a similar frequency and were well dispersed. The high number of gels that were positive for mitochondrial DNA most likely reflects the higher copy number of mitochondrial chromosomes relative to that of nuclear chromosomes within a cell.

Second screening for the presence of whole ATM locus amplicons

The nine gels that contained the *ATM* locus amplicon, including the two positive controls, were screened further for the entire *ATM* locus. Six additional loci were selected. Their PCR primer sequences (shown in Supplementary Table 1 in the supplementary material) span 240 kb of this region. Five gels (66, 71, and 91 and the two positive controls) were positive for all six loci. The remain-